Analysis of light extraction efficiency enhancement for thin-film-flip-chip InGaN quantum wells light-emitting diodes with GaN micro-domes

Peng Zhao and Hongping Zhao*

Department of Electrical Engineering and Computer Science, Case Western Reserve University, Cleveland, OH 44106, USA

*hongping.zhao@case.edu

Abstract: The enhancement of light extraction efficiency for thin-film flip-chip (TFFC) InGaN quantum wells (QWs) light-emitting diodes (LEDs) with GaN micro-domes on n-GaN layer was studied. The light extraction efficiency of TFFC InGaN QWs LEDs with GaN micro-domes were calculated and compared to that of the conventional TFFC InGaN QWs LEDs with flat surface. The three dimensional finite difference time domain (3D-FDTD) method was used to calculate the light extraction efficiency for the InGaN QWs LEDs emitting at 460nm and 550 nm, respectively. The effects of the GaN micro-dome feature size and the p-GaN layer thickness on the light extraction efficiency were studied systematically. Studies indicate that the p-GaN layer thickness is critical for optimizing the TFFC LED light extraction efficiency. Significant enhancement of the light extraction efficiency (2.5-2.7 times for λ_{peak} = 460nm and 2.7-2.8 times for λ_{peak} = 550nm) is achievable from TFFC InGaN QWs LEDs with optimized GaN micro-dome diameter and height.

OCIS codes: (230.3670) Light-emitting diodes; (230.0250) Optoelectronics.

References and links

1. S. Nakamura, M. Senoh, N. Iwasa, and S. Nagahama, "High-brightness InGaN blue, green and yellow light-emitting diodes with quantum well structures," Jpn. J. Appl. Phys. **34**(Part 2, No. 7A), L797–L799 (1995).
2. M. Krames, O. Shchekin, R. Mueller-Mach, G. Mueller, L. Zhou, G. Harbers, and M. Craford, "Status and future of high-power light-emitting diodes for solid-state lighting," IEEE J. Display Technol. **3**(2), 160–175 (2007).
3. M. H. Crawford, "LEDs for solid-state lighting: Performance challenges and recent advances," IEEE J. Sel. Top. Quantum Electron. **15**(4), 1028–1040 (2009).
4. N. Tansu, H. Zhao, G. Liu, X. H. Li, J. Zhang, H. Tong, and Y. K. Ee, "Breakthrough in photonics 2009: III-Photonics," IEEE Photonics J. **2**, 241–248 (2010).
5. I. H. Brown, P. Blood, P. M. Smowton, J. D. Thomson, S. M. Olaizola, A. M. Fox, P. J. Parbrook, and W. W. Chow, "Time evolution of the screening of piezoelectric fields in InGaN quantum wells," IEEE J. Quantum Electron. **42**(12), 1202–1208 (2006).
6. H. Zhao, G. Liu, J. Zhang, J. D. Poplawsky, V. Dierolf, and N. Tansu, "Approaches for high internal quantum efficiency green InGaN light-emitting diodes with large overlap quantum wells," Opt. Express **19**(S4 Suppl 4), A991–A1007 (2011).
7. R. A. Arif, Y. K. Ee, and N. Tansu, "Polarization engineering via staggered InGaN quantum wells for radiative efficiency enhancement of light emitting diodes," Appl. Phys. Lett. **91**(9), 091110 (2007).
8. H. Zhao, R. A. Arif, and N. Tansu, "Design analysis of staggered InGaN quantum wells light-emitting diodes at 500–540 nm," IEEE J. Sel. Top. Quantum Electron. **15**(4), 1104–1114 (2009).
9. H. Zhao, G. Liu, X.-H. Li, G. S. Huang, J. D. Poplawsky, S. T. Penn, V. Dierolf, and N. Tans, "Growths of staggered InGaN quantum wells light-emitting diodes emitting at 520–525 nm employing graded growth-temperature profile," Appl. Phys. Lett. **95**(6), 061104 (2009).
10. S. H. Park, D. Ahn, and J. W. Kim, "High-efficiency staggered 530 nm InGaN/InGaN/GaN quantum-well light-emitting diodes," Appl. Phys. Lett. **94**(4), 041109 (2009).
11. H. Zhao and N. Tansu, "Optical gain characteristics of staggered InGaN quantum wells lasers," J. Appl. Phys. **107**(11), 113110 (2010).
12. R. A. Arif, H. Zhao, and N. Tansu, "Type-II InGaN-GaNAs quantum wells for lasers applications," Appl. Phys. Lett. **92**(1), 011104 (2008).

#171268 - $15.00 USD Received 26 Jun 2012; revised 23 Aug 2012; accepted 27 Aug 2012; published 7 Sep 2012

13. H. Zhao, R. A. Arif, and N. Tansu, "Self-consistent gain analysis of type-II 'W' InGaN–GaNAs quantum well lasers," J. Appl. Phys. **104**(4), 043104 (2008).
14. S. H. Park, Y. T. Lee, and J. Park, "Optical properties of type-II InGaN/GaAsN/GaN quantum wells," Opt. Quantum Electron. **41**(11-13), 779–785 (2009).
15. H. Zhao, R. A. Arif, Y. K. Ee, and N. Tansu, "Self-consistent analysis of strain-compensated InGaN–AlGaN quantum wells for lasers and light-emitting diodes," IEEE J. Quantum Electron. **45**(1), 66–78 (2009).
16. C. L. Tsai, G. C. Fan, and Y. S. Lee, "Effects of strain-compensated AlGaN/InGaN superlattice barriers on the optical properties of InGaN light-emitting diodes," Appl. Phys., A Mater. Sci. Process. **104**(1), 319–323 (2011).
17. S. H. Park, Y. T. Moon, J. S. Lee, H. K. Kwon, J. S. Park, and D. Ahn, "Spontaneous emission rate of green strain-compensated InGaN/InGaN LEDs using InGaN substrate," Phys. Status Solidi., A Appl. Mater. Sci. **208**(1), 195–198 (2011).
18. J. Park and Y. Kawakami, "Photoluminescence property of InGaN single quantum well with embedded AlGaN δ layer," Appl. Phys. Lett. **88**(20), 202107 (2006).
19. S. H. Park, J. Park, and E. Yoon, "Optical gain in InGaN/GaN quantum well structures with embedded AlGaN δ layer," Appl. Phys. Lett. **90**(2), 023508 (2007).
20. H. Zhao, G. Liu, and N. Tansu, "Analysis of InGaN-delta-InN quantum wells for light-emitting diodes," Appl. Phys. Lett. **97**(13), 131114 (2010).
21. Y. Li, B. Liu, R. Zhang, Z. Xie, and Y. Zheng, "Investigation of optical properties of InGaN-InN-InGaN/GaN quantum-well in the green spectral regime," Physica E **44**, 821–825 (2012).
22. R. J. Choi, Y. B. Hahn, H. W. Shim, M. S. Han, E. K. Suh, and H. J. Lee, "Efficient blue light-emitting diodes with InGaN/GaN triangular shaped multiple quantum wells," Appl. Phys. Lett. **82**(17), 2764–2766 (2003).
23. S. H. Park, D. Ahn, and S. L. Chuang, "Electronic and optical properties of a- and m-plane Wurtzite InGaN/GaN quantum wells," IEEE J. Quantum Electron. **43**(12), 1175–1182 (2007).
24. A. Chakraborty, B. A. Haskell, S. Keller, J. S. Speck, S. P. Denbaars, S. Nakamura, and U. K. Mishra, "Demonstration of nonpolar m-plane InGaN/GaN light-emitting diodes on free-standing m-plane GaN substrates," Jpn. J. Appl. Phys. **44**(5), L173–L175 (2005).
25. H. Masui, S. Nakamura, S. P. DenBaars, and U. K. Mishra, "Nonpolar ands III-nitride light-emitting diodes: Achievements and challenges," IEEE Trans. Electron. Dev. **57**(1), 88–100 (2010).
26. C. Huh, K. S. Lee, E. J. Kang, and S. J. Park, "Improved light-output and electrical performance of InGaN-based light-emitting diode by microroughening of the p-GaN surface," J. Appl. Phys. **93**(11), 9383–9385 (2003).
27. T. Fujii, Y. Gao, R. Sharma, E. L. Hu, S. P. DenBaars, and S. Nakamura, "Increase in the extraction efficiency of GaN-based light-emitting diodes via surface roughening," Appl. Phys. Lett. **84**(6), 855–857 (2004).
28. J. J. Wierer, A. David, and M. M. Megens, "III-nitride photonic-crystal light-emitting diodes with high extraction efficiency," Nat. Photonics **3**(3), 163–169 (2009).
29. H. W. Choi, C. Liu, E. Gu, G. McConnell, J. M. Girkin, I. M. Watson, and M. D. Dawson, "GaN micro-light-emitting diode arrays with monolithically integrated sapphire microlenses," Appl. Phys. Lett. **84**(13), 2253–2255 (2004).
30. J. Q. Xi, H. Luo, A. J. Pasquale, J. K. Kim, and E. F. Schubert, "Enhanced light extraction in GaInN light-emitting diode with pyramid reflector," IEEE Photon. Technol. Lett. **18**(22), 2347–2349 (2006).
31. Q. Xi, M. F. Schubert, J. K. Kim, E. F. Schubert, M. Chen, S. Y. Lin, W. Liu, and J. A. Smart, "Optical thin-film materials with low refractive index for broadband elimination of Fresnel reflection," Nat. Photonics **1**, 176–179 (2007).
32. Y.-K. Ee, R. A. Arif, N. Tansu, P. Kumnorkaew, and J. F. Gilchrist, "Enhancement of light extraction efficiency of InGaN quantum wells light emitting diodes using SiO_2/polystyrene microlens arrays," Appl. Phys. Lett. **91**(22), 221107 (2007).
33. Y. K. Ee, P. Kumnorkaew, R. A. Arif, H. Tong, H. Zhao, J. F. Gilchrist, and N. Tansu, "Optimization of light extraction efficiency of III-Nitride LEDs with self-assembled colloidal-based microlenses," IEEE J. Sel. Top. Quantum Electron. **15**(4), 1218–1225 (2009).
34. O. B. Shchekin, J. E. Epler, T. A. Trottier, T. Margalith, D. A. Steigerwald, M. O. Holcomb, P. S. Martin, and M. R. Krames, "High performance thin-film flip-chip InGaN-GaN light-emitting diodes," Appl. Phys. Lett. **89**(7), 071109 (2006).
35. H. Kim, K. K. Kim, K. K. Choi, H. Kim, J. O. Song, J. Cho, K. H. Baik, C. Sone, Y. Park, and T.-Y. Seong, "Design of high-efficiency GaN-based light emitting diodes with vertical injection geometry," Appl. Phys. Lett. **91**(2), 023510 (2007).
36. S. Chang, W. Chen, S. Shei, C. Kuo, T. Ko, C. Shen, J. Tsai, W. Lai, J. Sheu, and A. Lin, "High-brightness InGaN-GaN power flip-chip LEDs," J. Lightwave Technol. **27**(12), 1985–1989 (2009).
37. C. Chu, F. Lai, J. Chu, C. Yu, C. Lin, H. Kuo, and S. Wang, "Study of GaN light-emitting diodes fabricated by laser lift-off technique," Appl. Phys. Lett. **95**, 3916–3922 (2004).
38. W. Y. Fu, K. K. Wong, and H. W. Choi, "Close-packed hemiellipsoid arrays: A photonic band gap structure patterned by nanosphere lithography," Appl. Phys. Lett. **95**(13), 133125 (2009).
39. P. Kumnorkaew, Y. K. Ee, N. Tansu, and J. F. Gilchrist, "Investigation of the deposition of microsphere monolayers for fabrication of microlens arrays," Langmuir **24**(21), 12150–12157 (2008).
40. C.-H. Chan, A. Fischer, A. Martinez-Gil, P. Taillepierre, C.-C. Lee, S.-L. Yang, C.-H. Hou, H.-T. Chien, D.-P. Cai, K.-C. Hsu, and C.-C. Chen, "Anti-reflection layer formed by monolayer of microspheres," Appl. Phys. B **100**(3), 547–551 (2010).
41. J. C. Hulteen and R. P. Vanduyne, "Nanosphere lithography: A materials general fabrication process for periodic particle array surfaces," J. Vac. Sci. Technol. A **13**(3), 1553–1558 (1995).

#171268 - $15.00 USD Received 26 Jun 2012; revised 23 Aug 2012; accepted 27 Aug 2012; published 7 Sep 2012

42. K. Yee, "Numerical Solution of Initial Boundary Value Problem Involving Maxwell's Equations in Isotropic Media," IEEE Trans. Antenn. Propag. **14**(3), 302–307 (1966).
43. M. Bass, *Handbook of Optics*, (Optical Society of America, **2**: Devices, Measurements, and Properties, 1994).
44. H. K. Cho, J. Jang, J. H. Choi, J. Choi, J. Kim, J. S. Lee, B. Lee, Y. H. Choe, K. D. Lee, S. H. Kim, K. Lee, S. K. Kim, and Y. H. Lee, "Light extraction enhancement from nano-imprinted photonic crystal GaN-based blue light-emitting diodes," Opt. Express **14**(19), 8654–8660 (2006).
45. D. H. Long, I. K. Hwang, and S. W. Ryu, "Design optimization of photonic crystal structure for improved light extraction of GaN LED," IEEE J. Sel. Top. Quantum Electron. **15**(4), 1257–1263 (2009).
46. S. L. Chuang, "Optical gain of strained wurtzite GaN quantum-well lasers," IEEE J. Quantum Electron. **32**(10), 1791–1800 (1996).
47. Y. S. Choi, M. Iza, E. Matioli, G. Koblmüller, J. S. Speck, C. Weisbuch, and E. L. Hu, "2.5λ microcavity InGaN light-emitting diodes fabricated by a selective dry-etch thinning process," Appl. Phys. Lett. **91**(6), 061120 (2007).
48. Y. C. Shen, J. J. Wierer, M. R. Krames, M. J. Ludowise, M. S. Misra, F. Ahmed, A. Y. Kim, G. O. Mueller, J. C. Bhat, S. A. Stockman, and P. S. Martin, "Optical cavity effects in InGaN/GaN quantum-well heterostructure flip-chip light-emitting diodes," Appl. Phys. Lett. **82**(14), 2221–2223 (2003).
49. D. G. Deppe and C. Lei, "Spontaneous emission and optical gain in a Fabry-perot microcavity," Appl. Phys. Lett. **60**(5), 527–529 (1992).
50. H. Benisty, H. De Neve, and C. Weisbuch, "Impact of planar microcavity effects on light extraction—Part I: Basic concepts and analytical trends," IEEE J. Quantum Electron. **34**(9), 1612–1631 (1998).
51. W. Lukosz, "Theory of optical-environment-dependent spontaneous emission rates for emitters in thin layers," Phys. Rev. B **22**(6), 3030–3038 (1980).

1. Introduction

As the promising candidate for the next generation lighting technology, light-emitting diodes (LEDs) play an important role in solid state lighting [1–4]. InGaN quantum wells (QWs) are employed as active region for LEDs emitting in the near ultraviolet, blue and green spectral region. However, major challenges still exist for high performance InGaN QWs LEDs, including 1) the existence of the spontaneous and piezoelectric polarizations in the III-nitride semiconductor materials [5] leads to the charge separation in the QWs, resulting in low radiative recombination rate of electrons and holes, and 2) low light extraction efficiency in InGaN QWs LEDs due to the total internal reflection at the semiconductor-air or semiconductor-encapsulant interface. Recently, approaches based on novel QWs designs have been proposed to engineer the band lineups of the InGaN QWs for enhancing the electron-hole wavefunction overlap, including the staggered InGaN QW [6–11], type-II InGaN-GaNAs QW [12–14], strain-compensated InGaN-AlGaN QW [15–17], InGaN-delta-AlGaN QW [18, 19], InGaN-delta-InN QW [20, 21], and triangular InGaN QW [22]. In addition, significant efforts have been focused on nonpolar / semipolar InGaN QWs growths for removing / reducing polarization field in the QW [23–25].

The limitation occurred in light extraction efficiency of III-nitride LEDs is attributed to the large refractive index difference between III-nitride semiconductor (n~2.4) and the ambient media [free space (n~1); epoxy resin (n~1.5)], which leads to severe total internal reflection at the interface. Most of the generated photons in the active region are trapped inside the LED device and finally absorbed by the material. In order to achieve high performance InGaN QWs LEDs with high total external quantum efficiency, the enhancement of the light extraction efficiency is crucial.

Recently, several approaches have been proposed for enhancing the light extraction efficiency of III-nitride LEDs, including surface roughness [26, 27], photonic crystal [28], patterned sapphire substrate [29], nanopyramids [30], graded refractive index material [31] and SiO_2/polystyrene microlens arrays [32, 33]. Potential issues such as non-uniformity, high cost, limited efficiency enhancement, material degradation and reliability are still required to be addressed in these approaches.

In this work, we studied the light extraction efficiency for the thin film flip-chip (TFFC) LEDs based on three-dimensional finite difference time domain (3D-FDTD) method. Light extraction efficiency of TFFC InGaN QWs LEDs with GaN micro-domes were calculated and compared to that of the conventional TFFC InGaN QWs LEDs with flat surface. Studies show that significant light extraction efficiency enhancement is achievable by optimizing both the bottom p-GaN layer thickness and the n-GaN micro-dome size.

#171268 - $15.00 USD Received 26 Jun 2012; revised 23 Aug 2012; accepted 27 Aug 2012; published 7 Sep 2012

2. TFFC InGaN QWs LEDs with GaN micro-domes

The light extraction efficiency of the following two TFFC InGaN QWs LEDs as shown in Fig. 1 was calculated by 3-D FDTD method. TFFC design has been widely used in the current commercial LEDs, which possesses high light extraction efficiency as compared to that of the conventional LED package [34–36]. Thin film LEDs could be realized by removing sapphire substrate by laser lift-off technique [37], while flip-chip LEDs are achieved by submounting the p-GaN on a high reflectance metallic mirror to form the vertical LED configuration, which allows the photons to emit from the n-GaN layer side, and allows flexible surface texturing and patterning process on relative thick n-GaN to enhance the extraction efficiency without the potential effect on InGaN QWs active region. The TFFC LEDs combine these two techniques, the 2D schematic of which is shown in Fig. 1(a).

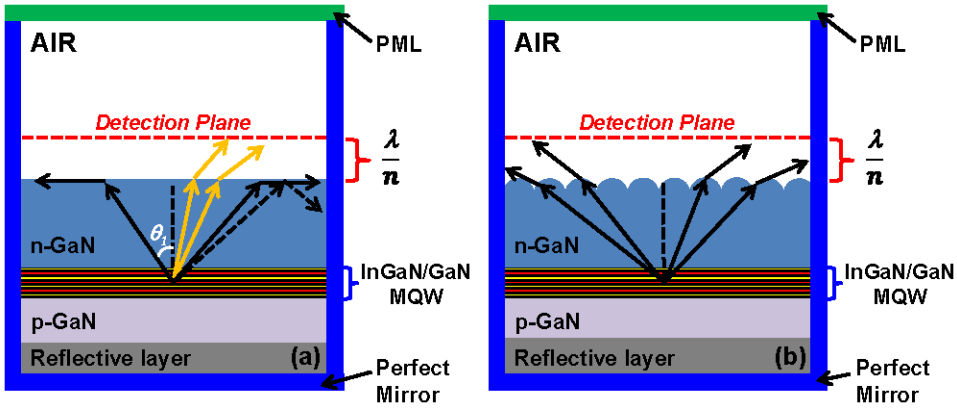

Fig. 1. 2D schematics of the thin film flip-chip (TFFC) InGaN QWs LEDs with (a) flat surface and (b) GaN micro-domes.

Here, we propose to form the GaN micro-domes on top of the n-GaN layer for enhancing the LED light extraction efficiency, as shown in Fig. 1(b). The GaN micro-domes could be formed by reactive ion etching (RIE) of the GaN layer with a self-assembled dielectric microspheres monolayer as mask. The spherical shape of the mask could be transferred to the GaN layer when the etching rates for both GaN and microspheres are comparable, which is achievable by optimizing the RIE condition [38]. The close-packed monolayer of dielectric microspheres could be deposited by using self-assembled approaches [39–41], such as rapid convective deposition [39], dip coating [40] and spin coating [41]. The TFFC InGaN QWs LED with GaN micro-domes [Fig. 1(b)] is based on the low cost self-assembled approach.

3. 3-D FDTD method for calculation of light extraction efficiency

3-D FDTD method was used to calculate the light extraction efficiency of the TFFC InGaN QWs LEDs with both flat surface and GaN micro-domes. The p-GaN layer thickness is critical for optimizing the light extraction efficiency due to the interference between the dipole source and the reflected waves from the bottom mirror. The effect of the micro-dome size on the light extraction efficiency was studied for the TFFC LEDs with GaN micro-domes. Note that the feature size of GaN micro-domes is in the range of submicron to micron, which is comparable to the wavelength emitted from InGaN QWs. As compared to the traditional approach based on ray tracing, the FDTD method is more accurate to solve the differential forms of Maxwell's equations with specific boundary conditions in such complex geometries.

In order to apply the Maxwell's equations by numerical method so as to realize FDTD calculation, Yee's mesh is used to enable analyzing the electromagnetic fields discretely in both space and time [42]. Figure 2 shows the unit cell of Yee's mesh grid, which involves positioning of the $\vec{E}$ and $\vec{H}$ in the cubic-cell space lattice with offset $n + 1$ and $n + 1/2$ (n is

#171268 - $15.00 USD Received 26 Jun 2012; revised 23 Aug 2012; accepted 27 Aug 2012; published 7 Sep 2012

integer), respectively. In three dimensions, the Maxwell's curl equations could be developed into the time-differentiated, spatial components in Cartesian coordinate system, which have six electromagnetic field components in each respective axis as shown in Fig. 2: E_x, E_y, E_z and H_x, H_y, H_z. All field components could be solved based on the set of differential form of Maxwell's equations. The spatial size of mesh is defined by Δx, Δy and Δz, which directly related to the simulation time and memory requirements in practical FDTD calculation. Based on this model, the Maxwell's equations are solved discretely in time, where the time step Δt here is defined by the mesh size through the speed of light. When the limit of mesh size goes to zero, the technique should be supposed to exactly represent the accurate calculation of Maxwell's equations.

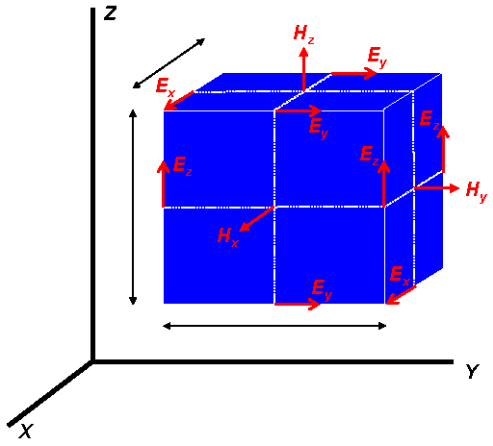

Fig. 2. Yee's mesh cell: Maxwell's equations are solved discretely in unit of Yee's mesh cell.

In this calculation, the loss from material absorption and the wavelength dependence of the refractive index $n(\lambda)$ are taken into account [43]. If we take the $\vec{E}$ along z direction as an example, the absorption in one unit Yee's mesh cell could be calculated as below:

$$E_z^{n+1} = \left(\frac{1-\sigma\Delta t/2\varepsilon}{1+\sigma\Delta t/2\varepsilon}\right)E_x^{n} + \left(\frac{2\Delta t/\Delta s}{2\varepsilon+\sigma\Delta t}\right)\left(\Delta H_y^{\,n+\frac{1}{2}} + \Delta H_x^{\,n+\frac{1}{2}}\right) \qquad (1)$$

where ε and σ are the permittivity and conductivity of the material, respectively.

Here, the lateral dimension of the computational domain is set as 10μm which is much smaller than that of the real LEDs (~300-1000μm). The boundary conditions for the four lateral boundaries as shown in Fig. 1 are set as perfect mirror to represent the limited lateral dimension as infinite [44, 45]. The reflections from the boundary perfect mirror takes into account the light extraction beyond the computational domain. With the perfect mirror lateral boundary conditions and the reflective layer at the bottom, photons emitted from the InGaN QWs and the light propagating after reflections can only be extracted out from the top n-GaN surface. The boundary condition for top simulation area is set as perfectly matched layer (PML) boundary condition, which absorbs electromagnetic energy incident upon it.

In the simulation, a single polarized dipole source is placed in the InGaN QWs active region, and the detection plane is set as $\lambda/n(\lambda)$ away from the emission surface of n-GaN, where λ represents the peak emission wavelength from the InGaN QWs and $n(\lambda)$ is the wavelength dependent refractive index of the media. The maximum mesh step is set as $\lambda/10*n(\lambda)$, and the average grid points are estimated around 1800000 in the computational domain, which generates good accuracy in the light extraction efficiency calculation.

#171268 - $15.00 USD Received 26 Jun 2012; revised 23 Aug 2012; accepted 27 Aug 2012; published 7 Sep 2012

The light extraction efficiency is defined as the ratio of total extracted light power to the total power emitted from InGaN QWs. In this simulation, the extracted power from TFFC LED surface can be obtained by integrating the Poynting vectors over far field projection surface, and the total power emitted from QWs were calculated by Poynting vectors integrated surrounding the near field of dipole source. The power integral equations can be expressed as:

$$\mathrm{E}(\omega) = \frac{1}{2}\int real\left(P(\omega)\right)dS \tag{2}$$

where $E(\omega)$ is the calculated energy, $P(\omega)$ is the Poynting vector depending on light angular frequency, and dS is the surface normal. In the far field, Poynting vectors could be calculated from electric field component $\vec{E}(\omega)$ based on the plane wave approximation, as follows:

$$P(\omega) = n(\omega)\sqrt{\frac{\varepsilon 0}{\mu_0}}\left|\vec{E}(\omega)\right|^2 \tag{3}$$

4. Results and discussions

4.1 Transverse Electric(TE) and Transverse Magnetic(TM) Components in InGaN QWs LEDs

In order to study the transverse electric (TE) and transverse magnetic (TM) components of the InGaN QWs spontaneous emission (R_{sp}), the calculations of the band structure and wavefunctions for InGaN QWs were carried out by using self-consistent 6-band ***k·p*** method for wurtzite semiconductors, taking into account the valence band mixing, strain effect, polarization fields, and carrier screening effect [15, 46].

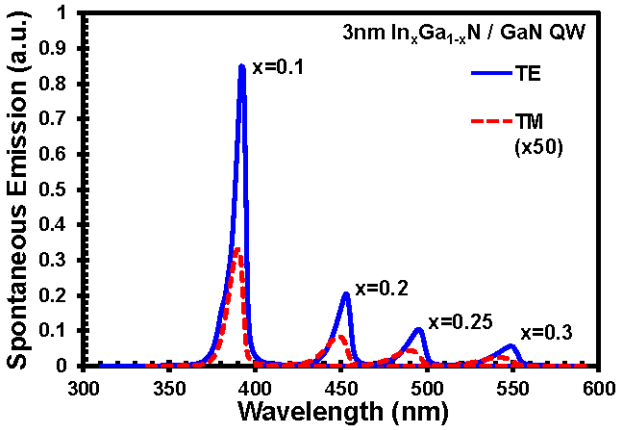

Fig. 3. Spontaneous emission spectra (TE component and TM component (x50)) for $In_xGa_{1-x}N$ QWs LEDs with x = 0.1, 0.2, 0.25 and 0.3.

Figure 3 plots the TE component and TM component (x50) of the spontaneous emission spectra for 3-nm $In_xGa_{1-x}N$ QWs with In-contents of x = 0.1, 0.2, 0.25 and 0.3, respectively. From Fig. 3, the TE spontaneous emission component dominates the total R_{sp} in the visible wavelength regime. In this calculation, the TE polarized dipole source is used for the light extraction efficiency calculation.

4.2 Effect of P-GaN layer thickness on light extraction efficiency for TFFC InGaN LEDs

Note that in the TFFC LEDs, the QWs active region is placed close enough to the reflective metallic mirror (on the order of 150-400 nm). The light emitted from QWs will interfere with the reflected waves, and the coupled interference patterns in the escape cone will lead to

#171268 - $15.00 USD Received 26 Jun 2012; revised 23 Aug 2012; accepted 27 Aug 2012; published 7 Sep 2012

significant changes in light extraction efficiency from conventional flip chip LEDs [48, 49]. In the FDTD calculations for conventional TFFC InGaN LEDs with flat surface, the distance between InGaN QWs active region and reflective layer could be modified by varying the p-GaN layer thickness, which is critical for optimizing the LED light extraction efficiency. Theoretical analysis on the optical cavity effects provides a reasonable model to analyze the dependence trend by calculating the monochromatic transmittance curve, in which the optical cavity is based on planar micro-cavity structure with a high-reflectance bottom mirror [50].

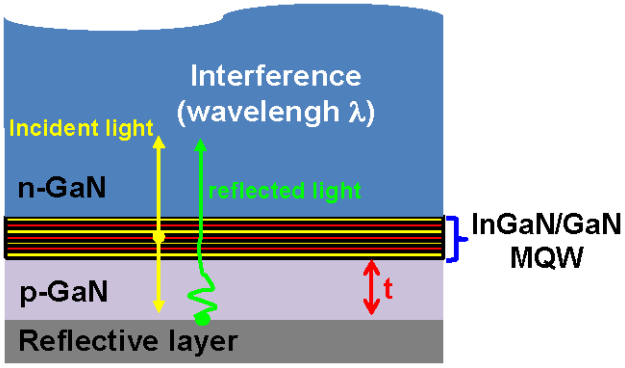

Fig. 4. Schematic of TFFC InGaN QWs LED with interference between emission of QWs and from bottom mirror.

As shown in Fig. 4, if a monochromatic oscillating dipole source with vacuum wavelength λ is located at a distance *t* above the bottom mirror, the interference patterns of the electric field upon dipole source and mirror could be expressed as follows [51]:

$$E^2(\omega) = E_0^2(\omega)\left|1 \pm r e^{2i\phi(\omega)}\right|^2 = E_0^2(\omega)\left(1 + r^2 \pm 2r\cos 2\phi(\omega)\right) \qquad (4)$$

where $E_0(\omega)$ is the electric field without mirror underneath, $\pm r$ is the amplitude reflectivity of bottom mirror, and $\phi(\omega)$ is the phase shift due to optical path difference, which is related to the source-mirror distance *t*, the incident angle θ (from the normal) and associated wave vector $k = \frac{2\pi n(\omega)}{\lambda}$. Note that half-cavity approximation is used here to assume the media thickness above the mirror is infinite. Also, the lifetime, polarization, and orientational effects of the dipole source are not taken into account for simplicity so as to get the upward-radiated electric far field from Eq. (4). Since phase shift upon the reflections off the mirror is neglected here, the total phase shift from optical path difference could be calculated as:

$$2\phi = 2kt\cos\theta \qquad (5)$$

Another approximation here is made to assimilate normal incident light ($\theta = 0$) and incident light within critical angle ($\theta < \theta_C$). For an dipole source located near bottom mirror, the phase changing difference for rays propagating between normal incidence and critical angle incident direction is trivial, hence $\cos\theta$ could assume to be 1 when $\theta < \theta_C$. Constructive interference coupling happens when $2kt = 2m\pi$ with integer *m* for + *r* and half-integer *m* for –*r*. Under perfect mirror approximation ($|r| = 1$) in Eq. (4), two constructive interference with + *r* and –*r* will bring the maximum ($E^2{}_{\max}(\omega) = 4E_0^2(\omega)$) and minimum ($E_{\min}(\omega) = 0$) electric field, respectively. Then the source-mirror distance *t* corresponding to

#171268 - $15.00 USD Received 26 Jun 2012; revised 23 Aug 2012; accepted 27 Aug 2012; published 7 Sep 2012

constructive interference between emitted light and reflected light could be achieved as follows:

$$t(\omega) = \frac{m\lambda}{2n(\omega)} \tag{6}$$

which indicates the periodicity of t is $\frac{\lambda}{2n(\omega)}$.

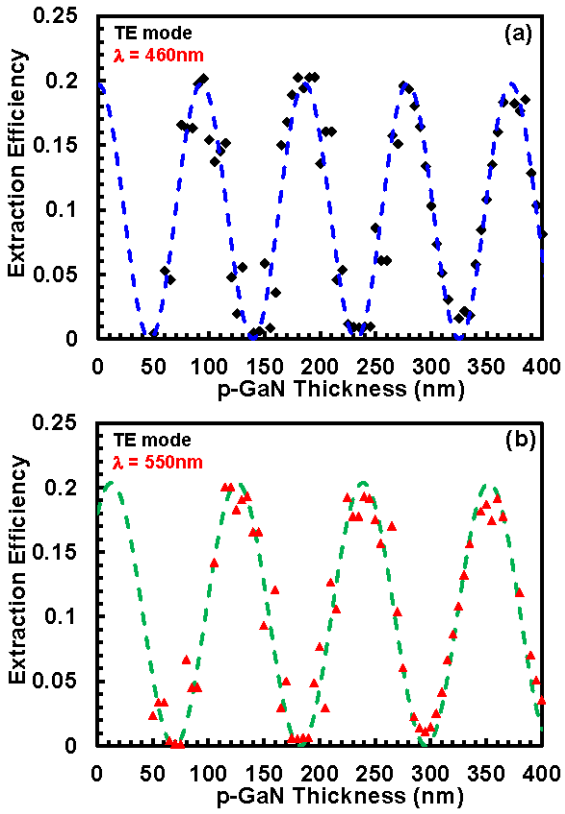

Fig. 5. Light extraction efficiency for the conventional TFFC InGaN QWs LEDs at wavelength (a) λ_{peak} = 460nm and (b) λ_{peak} = 550nm with flat surface as a function of the p-GaN layer thickness. N-GaN thickness is 2.5μm. Dash line and solid dots represent the theoretical fitting curve and the FDTD calculation results, respectively.

The dependence of the light extraction efficiency of TE polarized spontaneous emission component for the TFFC InGaN QWs LEDs on p-GaN layer thickness was calculated with wavelength of λ_{peak} = 460nm and λ_{peak} = 550nm, as shown in Fig. 5(a) and Fig. 5(b) respectively. The solid dots represent FDTD simulated results, and the dash line is the theoretical fitting curve, which was obtained from Eqs. (4) and (6) regarding oscillation periodicity and amplitude. In Fig. 5(a), the p-GaN layer thickness (t) periodicity calculated from Eq. (6) at λ_{peak} = 460nm is 92.9 nm and the peak light extraction efficiency amplitude is 0.198, which provides a good fitting to the solid dots obtained from FDTD calculation. In Fig. 5(b), the p-GaN layer thickness periodicity of t and light extraction efficiency amplitude corresponding to λ_{peak} = 550nm are 113.3 nm and 0.204 respectively, which also shows good agreement with the solid dots. Note that the complex refractive index of GaN used in the calculation is $2.48 + i1.3\text{x}10^{-3}$ (λ = 460nm) and $2.41 + i4.6\text{x}10^{-4}$ (λ = 550nm) [43].

#171268 - $15.00 USD Received 26 Jun 2012; revised 23 Aug 2012; accepted 27 Aug 2012; published 7 Sep 2012

From Fig. 5, the strong effect of the p-GaN layer thickness on the light extraction efficiency indicates the importance of optimizing the p-GaN thickness for the TFFC InGaN QWs LEDs. The peak light extraction efficiency and oscillation periodicity are determined by the emission wavelength and the material. The typical p-GaN layer thickness in InGaN QWs LEDs is around 200 nm. From Fig. 5, the optimized p-GaN layer thickness of 195 nm (λ_{peak} = 460nm) and 230nm (λ_{peak} = 550nm) were obtained for maximum light extraction of the conventional InGaN QWs TFFC LEDs with flat surface.

4.3 Effect of micro-dome (micro-hemisphere) size on light extraction efficiency for TFFC InGaN LEDs

In this work, the effects of the micro-dome diameter (*D*) and height (*h*) on the light extraction efficiency of the TE polarized spontaneous emission component were studied. Figure 6 plots the light extraction efficiency of the TFFC InGaN QWs LEDs with GaN micro-domes (h = D/2) as a function of the micro-dome diameter (*D*) at λ_{peak} = 460nm and λ_{peak} = 550nm. The optimized p-GaN layer thickness of 195 nm (λ_{peak} = 460nm) and 230nm (λ_{peak} = 550nm) were used in the calculation. The top n-GaN layer thickness is set as 2.5μm. Note that the extraction efficiency at D = 0 represents the case for conventional LEDs with flat surface. From Fig. 6, the LEDs with GaN micro-domes show significant enhancement of the light extraction efficiency at different micro-dome diameter. For emission wavelength of λ_{peak} = 460nm, the light extraction efficiency of LEDs with GaN micro-domes increases significantly from 0.209 (D = 0) to 0.476 (D = 500nm) and forms a peak at D = 500nm. Then the light extraction efficiency increases slightly and saturates (0.53) when D > 1μm. The light extraction efficiency of LEDs with GaN micro-domes for emission wavelength λ_{peak} = 550nm is also calculated for comparison. The result shows similar trend: it forms a peak with extraction efficiency of 0.477 at D = 600nm and saturates at 0.53 when D > 1.25μm.

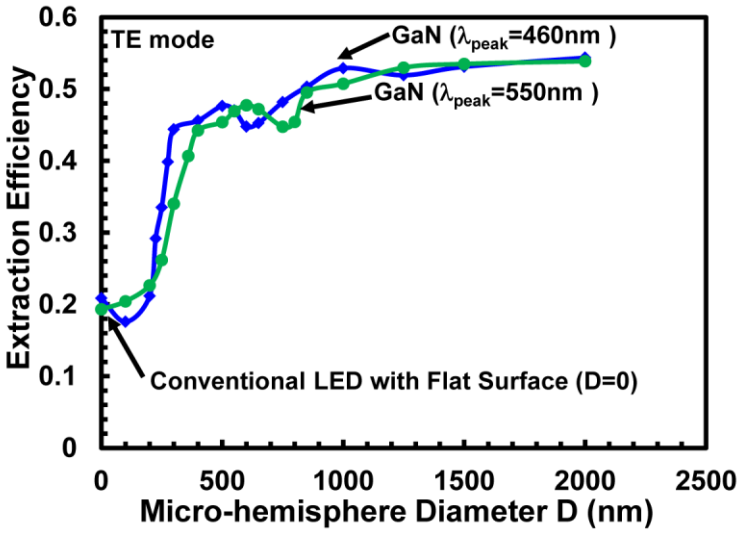

Fig. 6. Light extraction efficiency enhancement of TE polarized spontaneous emission component for TFFC InGaN QWs LEDs with optimized p-GaN thickness (195nm for λ_{peak} = 460nm, 230nm for λ_{peak} = 550nm as a function of GaN micro-hemisphere diameter (*D*).

Note that the light extraction efficiency of TFFC InGaN LEDs with GaN micro-domes as a function of the micro-dome diameter shows similar trend for emission wavelength of 460 nm and 550 nm. There exists a peak extraction efficiency value before the light extraction efficiency saturates at larger micro-dome diameter. The diameter corresponding to the peak light extraction efficiency shifts from D = 500 nm for λ_{peak} = 460nm to D = 600 nm for λ_{peak} = 550nm, which indicates its wavelength dependence characteristics. The maximum light

#171268 - $15.00 USD Received 26 Jun 2012; revised 23 Aug 2012; accepted 27 Aug 2012; published 7 Sep 2012

extraction efficiency enhancement of 2.6 times (λ_{peak} = 460nm) and 2.8 times (λ_{peak} = 550nm) are obtained from LEDs with GaN micro-domes when D~2μm.

For practical LED device fabrication, smaller size micro-domes are preferable due to 1) the short etching time required to form GaN micro-domes, and 2) less potential effect on InGaN QWs active region if the GaN micro-domes are distant from the QWs. Thus, the suitable micro-domes (h = D/2) for λ_{peak} = 460nm and λ_{peak} = 550nm are D = 1μm (2.53 times) and D = 1.25μm (2.74 times), respectively.

4.4 Effect of micro-dome size (micro-hemiellipsoid) on light extraction efficiency for TFFC InGaN LEDs

The light extraction efficiency of TFFC InGaN QWs LED with micro-domes was studied by tuning the micro-dome height *h* (h≠D/2). The studies indicate the optimized micro-dome structure for highest light extraction efficiency is not necessary from the micro-domes with h = D/2 (micro-hemisphere). Figure 7(a) shows the geometric structure of the general micro-dome structure on n-GaN layer, where h≠D/2. Figure 7(b) plots the light extraction efficiency of TFFC InGaN QWs LED with micro-dome structure as a function of the micro-dome height *h* for emission wavelength at λ_{peak} = 460nm.

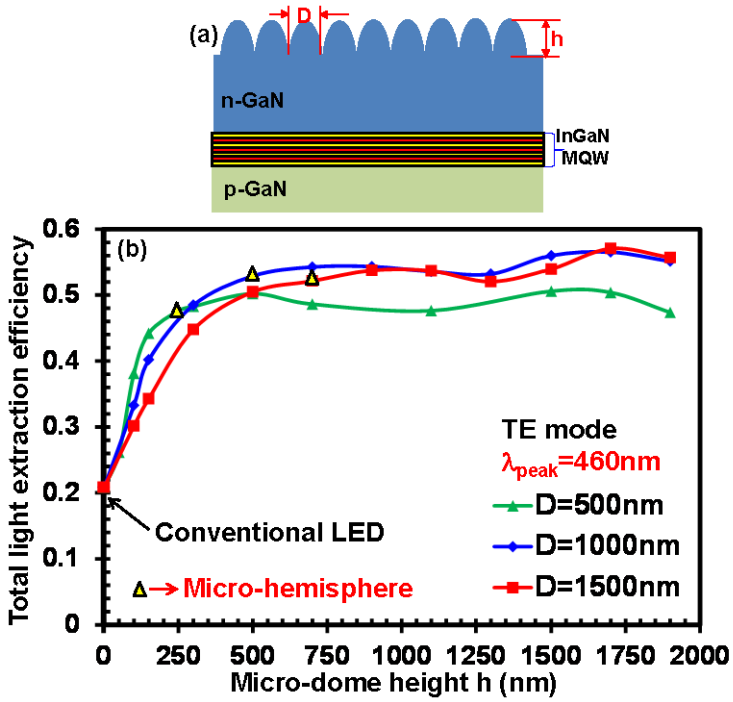

Fig. 7. (a) Geometric structure of the general micro-dome structure on n-GaN emission surface of TFFC InGaN QWs LED with diameter *D* and height *h*; (b) light extraction efficiency at λ_{peak} = 460nm from InGaN QWs TFFC LED with micro-dome structures as a function of micro-dome height h for diameters D = 500nm, D = 1000nm and D = 1500nm.

Three micro-dome diameter sizes D = 500nm, D = 1000nm and D = 1500nm were studied and plotted in Fig. 7(b). Note that the yellow triangular dot on each curve indicates the light extraction efficiency with micro-hemisphere structure (h = D/2). The light extraction efficiency at h = 0 represents the case for the conventional LED with flat surface. From Fig. 7(b), the optimized micro-dome structure for highest light extraction efficiency occurs at h>D/2. For TFFC InGaN QWs LEDs with GaN micro-domes emitting in the visible wavelength region, the light extraction efficiency could be optimized by tuning both the diameter and the height of the micro-domes. The enhancement of 2.71 times was achieved at

#171268 - $15.00 USD Received 26 Jun 2012; revised 23 Aug 2012; accepted 27 Aug 2012; published 7 Sep 2012

λ_{peak} = 460nm when D = 1μm and h = 1.7μm. In practical devices, the aspect ratio of the GaN micro-domes is not required to be accurately controlled to form exact micro-hemisphere shape, which provides tolerance for device fabrication.

4.5 P-GaN layer thickness dependence of light extraction efficiency for TFFC InGaN QWs LEDs

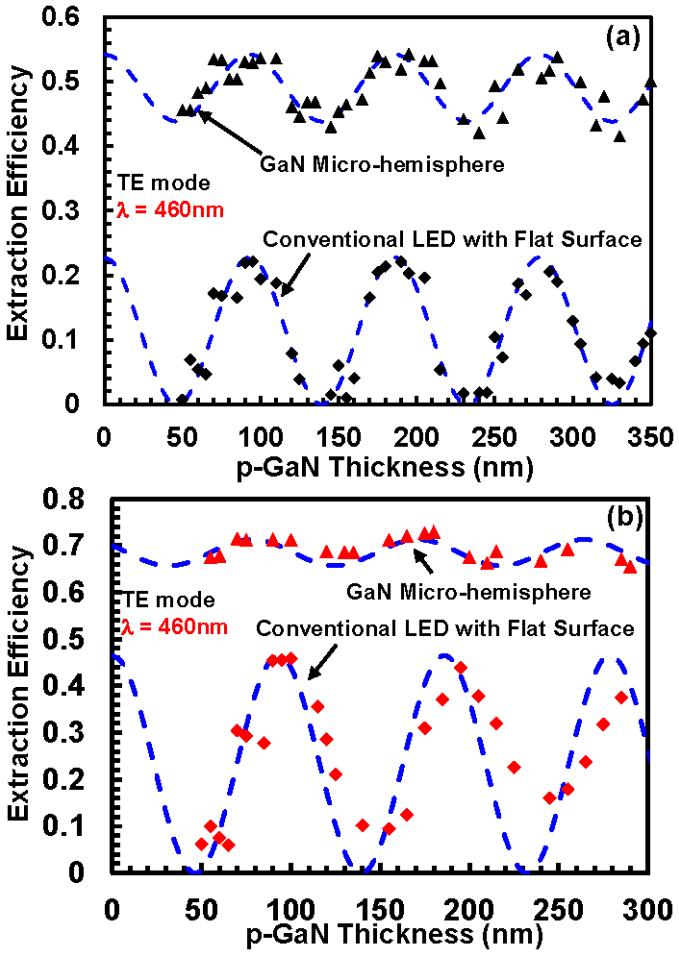

Fig. 8. Light extraction efficiency for the conventional TFFC InGaN QWs LEDs (λ_{peak} = 460nm) with flat surface and with GaN micro-domes as a function of the p-GaN layer thickness assuming the ambient medium is (a) air (n = 1), and (b) epoxy resin (n~1.5). Dash lines and solid dots represent the theoretical fitting curves and the FDTD calculation results, respectively.

The light extraction efficiency dependence on the p-GaN layer thickness for the TFFC InGaN QWs LEDs with 1 μm diameter of GaN micro-domes was calculated and plotted, as shown in Fig. 8. Figure 8(a) calculated the case that assumes the ambient medium is air (n = 1), and Fig. 8(b) calculated the case that assumes the ambient medium is epoxy resin (n~1.5), which is widely used in the current LEDs. For both cases, the periodic oscillations of the light extraction efficiency as a function of the p-GaN layer thickness for the conventional TFFC InGaN QWs LEDs with flat surface were also plotted for comparison. The results show good agreement between the theoretical fitting curves (dash lines) and the FDTD simulation results (triangular dots) for the TFFC InGaN LEDs.

#171268 - $15.00 USD Received 26 Jun 2012; revised 23 Aug 2012; accepted 27 Aug 2012; published 7 Sep 2012

Note that the LED with GaN micro-domes show significant light extraction efficiency enhancement at different p-GaN layer thickness as compared to that of the conventional LED. The light extraction efficiency for the LEDs with micro-domes also oscillates as a function of the p-GaN layer thickness, but with smaller amplitude of oscillation as compared to that of the conventional LEDs, which is due to the enhancement of the light escape cone from the GaN micro-domes. In conventional LEDs with flat surface and limited light escape cone, when the p-GaN layer thickness leads to a destructive interference within the escape cone, the constructive interference exists beyond the photon escape cone, which results in extremely low light extraction efficiency. In LEDs with GaN micro-domes and p-GaN thickness for destructive interference, the increase of the light escape cone leads to light extraction efficiency enhancement of the constructive interference, which is otherwise trapped inside the semiconductor in conventional LEDs with narrow light escape cone. This indicates the TFFC LED light extraction efficiency has weaker dependence on the p-GaN layer thickness by employing the GaN micro-domes.

For practical conventional TFFC InGaN LED epitaxy, the p-GaN layer thickness is required to be precisely controlled in order to obtain the maximum light extraction efficiency. By employing GaN micro-domes, it provides more tolerance for the p-GaN layer growth. The use of GaN micro-domes contributes higher light extraction efficiency in a wider range of p-GaN layer thickness.

5. Conclusion

The light extraction efficiency for TFFC InGaN QWs LEDs was studied by using 3-D FDTD method. TFFC InGaN QWs LEDs with GaN micro-domes on top of n-GaN layer show significant enhancement of light extraction efficiency. The optimized light extraction efficiency enhancement of 2.5-2.7 times (λ_{peak} = 460nm) and 2.7~2.8 times (λ_{peak} = 550nm) for LEDs with GaN micro-domes were achieved with micro-dome size of D~1μm and h~0.5-1.7 μm (λ_{peak} = 460nm) and D~1.25μm, h~0.625μm (λ_{peak} = 550nm). The design of the LEDs with GaN micro-domes has great potential to significantly enhance the total light extraction efficiency of the TFFC InGaN QWs LEDs and allows more tolerance in p-GaN layer growth thickness, which in turn leads to enhancement of the total external quantum efficiency of InGaN QWs LEDs in a wider range of p-GaN layer thickness.

Acknowledgment

The authors acknowledge financial support through start-up funds from Case Western Reserve University.

#171268 - $15.00 USD Received 26 Jun 2012; revised 23 Aug 2012; accepted 27 Aug 2012; published 7 Sep 2012